

VUV-luminescence and excitation spectra of the heavy trivalent rare earth ions in fluoride matrices

© M. Kirm^{*,**}, V.N. Makhov^{***}, M. True^{*}, S. Vielhauer^{*}, G. Zimmerer^{*}

^{*} Institut für Experimentalphysik, University of Hamburg,
D-22761 Hamburg, Germany

^{**} Institute of Physics, University of Tartu,
51014 Tartu, Estonia

^{***} P.N. Lebedev Physical Institute, Russian Academy of Sciences,
119991 Moscow, Russia

E-mail: georg.zimmerer@desy.de

VUV $4f^n \rightarrow 4f^{n-1}5d$ transitions of Gd^{3+} , Er^{3+} , Tm^{3+} , and Lu^{3+} in fluoride matrices have been analysed with high-resolution luminescence and excitation spectroscopy. In trifluorides, strong electron-phonon coupling has been found. In the other matrices, the luminescence spectra clearly yield zero-phonon lines and phonon replica, indicating intermediate coupling. The energies of the zero-phonon lines observed are compared with theoretical predictions. Near the threshold of $f \rightarrow d$ excitations, some of the excitation spectra yield sharp structures which cannot be explained with phonon replica but will be discussed in terms of the energy levels of the $4f^{n-1}5d$ configuration.

The work was supported by the Minister of Science and Technology of Germany under contracts 05 KS1GUD/1 and 03N8019D. Support by the Graduiertenkolleg Felder und lokalisierte Atome–Atome und lokalisierte Felder of the Deutsche Forschungsgemeinschaft (GRK 403) is gratefully acknowledged.

1. Introduction

Already of 1966, $4f^n \rightarrow 4f^{n-1}5d$ transitions of trivalent rare earth (RE^{3+}) ions in a CaF_2 matrix were reported [1]. Except for Ce^{3+} and Pr^{3+} , the transition energies are in the vacuum ultraviolet (VUV) range. In the past, the VUV $4f^n \rightarrow 4f^{n-1}5d$ transitions did not attract as much attention as the $4f^n \rightarrow 4f^{n-1}4f^*$ transitions because no application was in sight. In recent years, however, $4f^n \rightarrow 4f^{n-1}5d$ transitions gained much interest, being an essential aspect of quantum cutting phosphors [2].

Concerning the experimental difficulties in VUV spectroscopy, the pioneering work of Yen et al. [3] demonstrated the potential of synchrotron radiation (SR) for luminescence experiments. It was applied for the first time to RE^{3+} $4f^n \rightarrow 4f^{n-1}5d$ excitations by Elias et al. and Heaps et al. [4,5]. The first $4f^{n-1}5d \rightarrow 4f^n$ VUV luminescence spectra of Nd^{3+} , Er^{3+} , and Tm^{3+} were published by Yang and DeLuca [6]. For the first half of the lanthanide series, transitions from the lowest $4f^{n-1}5d$ level into the $4f^n$ ground state are spin-allowed with short lifetimes (up to ≈ 50 ns). In the second half, such transitions are spin-forbidden (lifetimes in the μs -range). Depending on the ion and the host, spin-forbidden emission from the lowest high-spin and spin-allowed emission from the lowest low-spin $4f^{n-1}5d$ state co-exist [2,7]. In the past, VUV RE^{3+} emission has been detected only from Nd^{3+} , Er^{3+} , and Tm^{3+} [2,7–10].

RE^{3+} $4f^{n-1}4f^*$ excitations couple weakly to the lattice because the $4f$ wave functions are shielded by the filled $5s$ and $5p$ shells. The $5d$ wave functions are more extended. Therefore, $4f^{n-1}5d$ excitations are expected to interact stronger with the lattice. The VUV $d \rightarrow f$ emission bands observed in the past were broad, nearly Gaussian shaped,

indicating at first sight strong coupling. However, already Schlesinger and Szczurek [11] observed zero-phonon lines (ZPLs) in $f \rightarrow d$ absorption spectra. Wegh et al. [2] found ZPLs also in luminescence excitation spectra and pointed out that the smooth shape of the emission bands originates from rather poor spectral resolution. SR excited experiments recording high-resolution spectra were missing until recently [12]. In the meantime, laser-excited spectra have been reported as well [13,14]. In the present paper, high-resolution spectra of $d \rightarrow f$ luminescence of Er^{3+} [12] and Tm^{3+} [14] will be discussed. The first $d \rightarrow f$ spectra of Gd^{3+} and Lu^{3+} [15] will be presented as well. Gd^{3+} is of particular interest because Gd^{3+} $d \rightarrow f$ emission was not expected at all for reasons given below. The sample include RE^{3+} doped fluorides and stoichiometric fluorides. Strong and intermediate coupling was established. The results agree well with predictions based on papers by Dorenbos [16,17].

2. Experiment

Most of the experiments were performed under selective SR excitation at the SUPERLUMI set-up at HASYLAB (Hamburg) [18]. The resolution intervals in excitation $\Delta\lambda_{ex}$ have been chosen between 3 and 0.5 \AA . The time structure of SR with its short pulses (width 150 ps) at a repetition rate between 1 and 5 MHz is the basis of time-resolved spectroscopic methods [19]. High-resolution VUV luminescence analysis was performed with a 1 m monochromator equipped with a position sensitive channel-plate detector. Most spectra were recorded in first order with $\Delta\lambda_{em} \approx 1 \text{ \AA}$. In some cases, luminescence analysis was carried out in second order ($\Delta\lambda_{em} \approx 0.5 \text{ \AA}$). In most of the experiments, the temperature was near LHe temperature (7–10 K).

For excitation spectra of VUV luminescence, the Pouey-type VUV monochromator of SUPERLUMI has been used to select the respective emission band. This monochromator has a large f -number (2.8), however, at the expense of spectral resolution ($\Delta\lambda_{\text{em}} = 10\text{--}20 \text{ \AA}$). Therefore, in the spectral range of ZPLs, scattered light from excitation falsifies the spectra. In the case of spin-forbidden $d \rightarrow f$ emission with its long lifetime, the spectra can be measured in the time-resolved mode, recording the emission within a time-window avoiding any contribution of the (prompt) scattered light of excitation. Spin-allowed emission, however, strongly overlaps in time with the scattered light. Therefore, discrimination between both contributions is difficult. Some experiments were performed under soft X-ray excitation at the undulator beamline BW3 of HASYLAB, where luminescence was analyzed with $\Delta\lambda_{\text{em}} = 6 \text{ \AA}$.

Tm³⁺ doped crystals have also been investigated under F₂-laser excitation ($157.6 \text{ nm}/63\,452 \text{ cm}^{-1}$) at the University of Utrecht [14]. The spectra yield an excellent signal-to-noise ratio. The spectral resolution of $f \rightarrow f$ spectra under laser excitation exceeds the one available at the SUPERLUMI station at least by a factor of 2. In the VUV, a comparable resolution is achieved at both setups. Laser excitation is superior to SR excitation in those cases where the excitation wavelength fits the requirements. However, VUV excitation spectra which presently can be measured only with SR, are of similar importance. Both excitation sources are complementary and should be used in parallel for the spectroscopy of RE³⁺ VUV $d \rightarrow f$ luminescence.

3. Results and discussion

3.1. Er³⁺ $d \rightarrow f$ luminescence. LiYF₄:Er³⁺ was chosen as a model for two reasons, (i) there exists only one site for the RE ion, and (ii) all kinds of Er³⁺

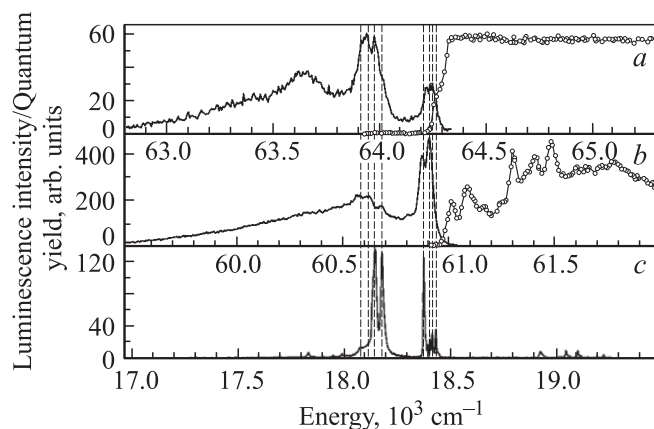


Figure 1. Spin-allowed (a), spin-forbidden (b), and ${}^4S_{3/2} \rightarrow {}^4I_{15/2}\text{Er}^{3+} f \rightarrow f$ luminescence (c) of LiYF₄:Er³⁺ (1%) at $T = 6 \text{ K}$. The bars indicate the Stark levels of the ${}^4I_{15/2}$ ground state with $2|M_J| = 5, 15, 3, 1, 9, 7, 11, 13$ [21] (from the right to the left). The resolution intervals are $\Delta\lambda_{\text{ex}} = 0.6 \text{ \AA}$ and $\Delta\lambda_{\text{em}} = 0.6 \text{ \AA}$.

luminescence co-exist. Moreover, the Stark splitting of the $4f^{11}{}^4I_{15/2}$ ground state is known with high accuracy (8 Stark levels) [20,21]. This is an essential condition for an analysis of the high-resolution spectra. In Fig. 1, the $d \rightarrow f$ luminescence spectra of LiYF₄:Er³⁺ (1%) are shown. They yield narrow lines and broad side bands. For comparison, the excitation spectrum of the spin-forbidden $d \rightarrow f$ emission is plotted as well. The relative calibration in excitation and in emission is correct within $\pm 0.2 \text{ \AA}$ ($\pm 8 \text{ cm}^{-1}$ at $64\,000 \text{ cm}^{-1}$). The $d \rightarrow f$ emission is compared with LiYF₄:Er³⁺ (1%) ${}^4S_{3/2} \rightarrow {}^4I_{15/2}$ emission. The bars correspond to an assignment of the ${}^4S_{3/2}$ emission lines to the Stark levels of the ground state [20,21]. ${}^4S_{3/2}$ emission was positioned with respect to the $d \rightarrow f$ emissions in order to obtain the best agreement with the lines in the $d \rightarrow f$ spectra.

The emission and excitation spectra being in scale, we are able to compare the sharp structures with the bars. In the spin-allowed case, the Stark level $2|M_J| = 5$ (the only one being populated at LHe temperature!) agrees with the shoulder at the low-energy onset of excitation ($64\,265 \text{ cm}^{-1}$). This shoulder is ascribed to the ZPL in excitation, being strongly suppressed by re-absorption. In emission, the respective ZPL is also indicated by a shoulder. The sharp structures at lower energy correspond to bars indicating the Stark levels of the ground state. They are ascribed to ZPLs as well. In the spin-forbidden case, the bar $2|M_J| = 5$ is energetically below the first maximum of the excitation spectrum at $61\,013 \text{ cm}^{-1}$. Provided this maximum arises from the ZPL in excitation there is a shift of the order of 60 cm^{-1} between excitation and emission, indicating an emission originating from disturbed centres. In the spin-forbidden case not all lines are resolved. This may indicate a variety of disturbed centres.

Phonon side-bands are not clearly resolved. As an estimate of the effective phonon energy, $\omega_{\text{eff}} = 330 \text{ cm}^{-1}$ measured by Renfro et al. [22] for the coupling of f levels to the LiYF₄ host may be considered. Then, the first side bands of the ZPLs with $2|M_J| = 5, 15, 3, 1$ are expected to overlap with the second group of ZPLs. The second group of phonon side bands of the ZPLs $2|M_J| = 5, 15, 3, 1$ would roughly coincide with the first group of side bands of the ZPLs $2|M_J| = 9, 7, 11, 13$. This may explain the maximum at $63\,650 \text{ cm}^{-1}$ (spin-allowed) and the shoulder at $60\,350 \text{ cm}^{-1}$ (spin-forbidden).

In Fig. 2, excitation spectra are presented in the range of the lowest spin-forbidden and spin-allowed $f \rightarrow d$ excitations. An excitation spectrum of ${}^4S_{3/2} \rightarrow {}^4I_{15/2}$ emission is included for comparison. In the spin-allowed case, the spectrum has a fast rise (with the shoulder discussed above) to a flat plateau. The plateau arises from total absorption (saturation). In the spin-forbidden case, saturation is not reached, but a fine structure is observed. At first sight, it seems straightforward to ascribe the structures to vibronic sidebands. Note, however, the maxima in the excitation spectrum have no counterpart in the spin-forbidden $d \rightarrow f$ emission. Therefore, phonon replica cannot account for

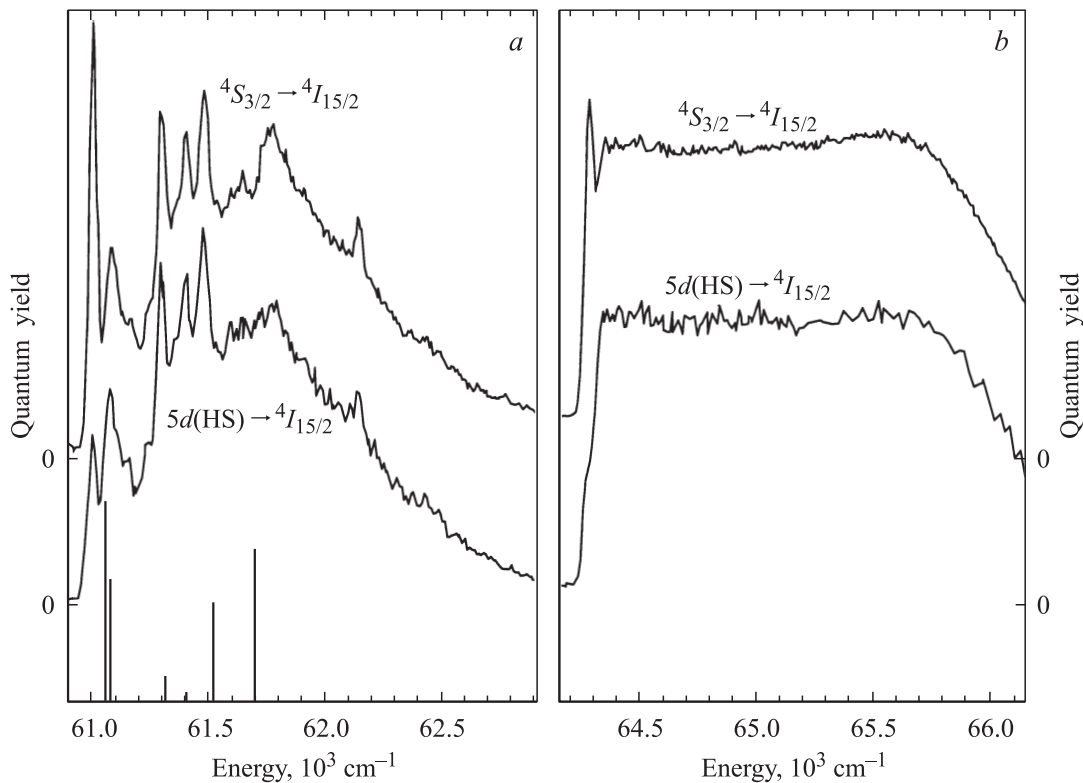


Figure 2. Excitation spectra of the spin-forbidden $\text{LiYF}_4:\text{Er}^{3+}$ (1%) $d \rightarrow f$ and of ${}^2S_{3/2} \rightarrow {}^4I_{15/2}$ emission at the onset of spin-forbidden (a) and spin-allowed (b) $f \rightarrow d$ excitation. $T = 9\text{ K}$, $\Delta\lambda_{\text{ex}} = 0.6\text{ \AA}$.

the fine structure. It originates from a coupling of the d excitations with the f^{10} core of the Er^{3+} ion. Pieterse et al. calculated the energy levels of the $\text{Er}^{3+} 4f^{10}5d$ configuration [23]. In Fig. 2, the respective energy levels are indicated by bars. The height of a bar is a relative measure of the oscillator strength. The numerical values were communicated to us by Meijerink [24].

Concerning the peak positions, good agreement is found between the calculated levels and the maxima of the excitation spectrum. The peaks represent the ZPLs in excitation for the spin-forbidden $4f^{10}5d$ levels. The relative heights, however, are in disagreement with experiment. This is explained as follows. Like in luminescence, each ZPL is accompanied by phonon sidebands, merging together to a background in the excitation spectrum. The spin-forbidden $d \rightarrow f$ emission of $\text{LiYF}_4:\text{Er}^{3+}$ has also been measured by Peijzel [13], in good agreement with the results of Ref. [12].

3.2. $\text{Tm}^{3+} d \rightarrow f$ luminescence. $\text{Tm}^{3+} d \rightarrow f$ emission has been investigated in LiCaAlF_6 (LiCAF). The choice of LiCAF was motivated by the fact that this matrix offers a divalent and a trivalent site, which makes it a promising candidate for co-doping with a RE^{3+} and a divalent ion as in Mn^{2+} doped LiSrAlF_6 [25]. Fig. 3 shows VUV emission spectra of $\text{LiCAF}:\text{Tm}^{3+}$ (0.04%) with a fine structure, merging into a smooth wide band. At first sight it may be tempting to ascribe the fine structure to $f \rightarrow f$ transitions. However, in the respective energy

range, the Tm^{3+} ion has no f levels [26]. In particular, the 1S_0 level at $\sim 75\,000\text{ cm}^{-1}$ [26,27] cannot contribute to the spectra shown (note also, both excitation energies are well below the 1S_0 level). At LHeT, the emission has a lifetime $\tau = 7\text{ }\mu\text{s}$ [14]. Therefore, it is ascribed to the spin-forbidden transition into the 3H_6 ground state. Only spin-forbidden $d \rightarrow f$ emission was observed, whereas other systems also emit spin-allowed luminescence [7,8]. In view of the low Tm^{3+} concentration, weak spin-allowed $d \rightarrow f$ luminescence in LiCAF cannot be excluded.

Compared to $\text{LiYF}_4:\text{Er}^{3+}$, the Tm^{3+} doped system is more complicated. Depending on the symmetry of the site, up to 13 Stark levels can exist for the 3H_6 ground state. In order to get more insight into the origin of the fine structure, a spectrum of the ${}^1G_4 \rightarrow {}^3H_6$ luminescence around $21\,000\text{ cm}^{-1}$ was plotted in Fig. 3 for comparison. The scales were arranged in a way that the sharp lines with the highest energies coincide. True [14] tentatively assigned the sharp structures in the ${}^1G_4 \rightarrow {}^3H_6$ spectrum to 12 Stark levels, covering a range of $\sim 400\text{ cm}^{-1}$. In the context of the present paper this means that the peaks in the $d \rightarrow f$ spectra below $61\,000\text{ cm}^{-1}$ cannot originate from ZPLs. They are ascribed to vibronic side bands. Only the sharp maxima above $\sim 61\,000\text{ cm}^{-1}$, in particular the one at $61\,410\text{ cm}^{-1}$, originate from ZPLs. The assignment of the peak at $61\,410\text{ cm}^{-1}$ is further supported by an analysis of the spin-forbidden $d \rightarrow f$ emission terminating at 3F_4

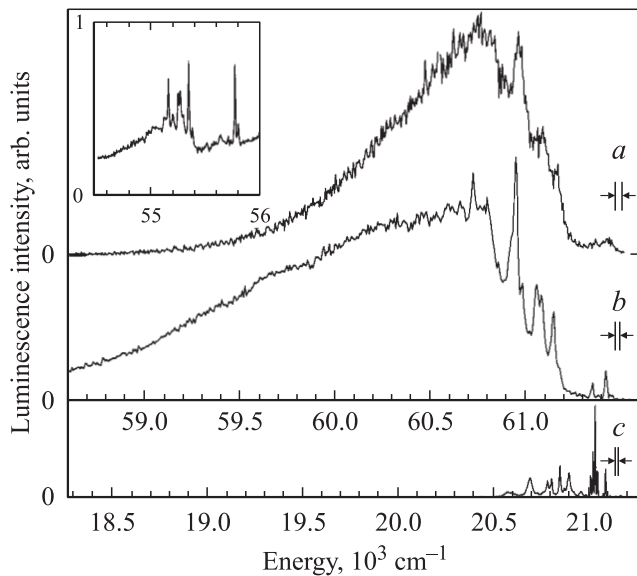


Figure 3. Spin-forbidden $d \rightarrow f$ luminescence of Tm^{3+} in LiCaAlF_6 . (a) SR excitation at $67\,659\text{ cm}^{-1}$, $\Delta\lambda_{\text{em}} = 0.8\text{ \AA}$, $T = 7.4\text{ K}$; (b) laser excitation at $63\,452\text{ cm}^{-1}$, $\Delta\lambda_{\text{em}} = 0.3\text{ \AA}$, $T = 7.3\text{ K}$; (c) $^1G_4 \rightarrow ^3H_6$ luminescence in $\text{LiCaF}_6:\text{Tm}^{3+}, \text{Mn}^{2+}$, laser excitation like in (b), $\Delta\lambda_{\text{em}} = 0.8\text{ \AA}$, $T = 7.3\text{ K}$.

(inset of Fig. 3). Two closely spaced peaks at $55\,797$ and $55\,766\text{ cm}^{-1}$ were observed, having an energy difference to the first ZPL terminating at 3H_6 of 5613 cm^{-1} and 5644 cm^{-1} , respectively. These energies coincide well with the energy of the first excited f state in $\text{LaF}_3:\text{Tm}^{3+}$ at 5615 cm^{-1} [26], a value that hardly changes in different matrices. Both peaks may be due to electronic transitions to closely spaced Stark levels of 3F_4 , however, they can be as well due to ZPLs of Tm^{3+} on different occupational sites.

3.3. $\text{Gd}^{3+} d \rightarrow f$ luminescence. The case of Gd^{3+} is of special interest because $\text{Gd}^{3+} d \rightarrow f$ emission was not expected at all due to the fact that the $4f^7$ energy levels are very dense at higher energies [13,28]. Such a dense level system is an ideal acceptor for energy transfer from d excitations and subsequent non-radiative relaxation into the emitting f levels of Gd^{3+} , thus quenching radiative $d \rightarrow f$ transitions. Nevertheless, the final answer is given by an experiment. In Fig. 4, VUV luminescence spectra of Gd^{3+} ions in LiGdF_4 and GdF_3 are presented [15]. At $T = 10\text{ K}$, the following lifetimes were measured, $\tau = 2.8\text{ ns}$ (LiGdF_4) and $\tau = 0.97\text{ ns}$ (GdF_3) [15]. The luminescence observed is ascribed to spin-allowed $\text{Gd}^{3+} d \rightarrow f$ emission. The arguments are as follows.

(i) The emission is clearly correlated to $\text{Gd}^{3+} 4f^7 \rightarrow 4f^65d$ excitation (see below).

(ii) In the case of GdF_3 , in spite of the high spectral resolution, only a broad band is observed which is typical for strong coupling to the lattice, excluding an $f \rightarrow f$ nature of the emission. In the case of LiGdF_4 , sharp lines and a broad sideband are observed. This is typical for intermediate coupling.

(iii) There is good agreement with an estimate of the transition energies according to the phenomenological approach by Dorenbos [16,17].

As already mentioned, the Gd^{3+} results are really unexpected. In order to demonstrate why, we included in Fig. 4 recently calculated $4f$ energy levels of the Gd^{3+} ion in LaF_3 which should be a good approximation to the case of $\text{LiYF}_4:\text{Gd}^{3+}$ [24]. The levels are all doublet or quartet levels whereas the emitting d level is an octet level. Therefore, non-radiative transitions from the emitting d level to these high-lying f levels are highly spin-forbidden. This may qualitatively explain why the emitting d level is not quenched by the f levels. In this context, we would like to point out that the $\text{Gd}^{3+} d \rightarrow f$ luminescence is thermally quenched, disappearing near 200 K .

We have to discuss now the fine structure of Gd^{3+} emission. Contrary to the case of Er^{3+} , the level structure of the $\text{Gd}^{3+} ^8S_{7/2}$ ground state is simple (no Stark splitting in first order) and only one ZPL is expected. The fine structures may arise from (i) phonon side bands, (ii) site effects, or (iii) a mixture of both. More insight could be obtained from excitation spectra. In the stoichiometric as well as in $\text{LiYF}_4:\text{Gd}^{3+}$ (10%), in the range of allowed excitations the sample is optically thick, thus preventing an analysis of the spectral shape of absorption. What can be done, however, is doping the crystal with another RE^{3+} ion

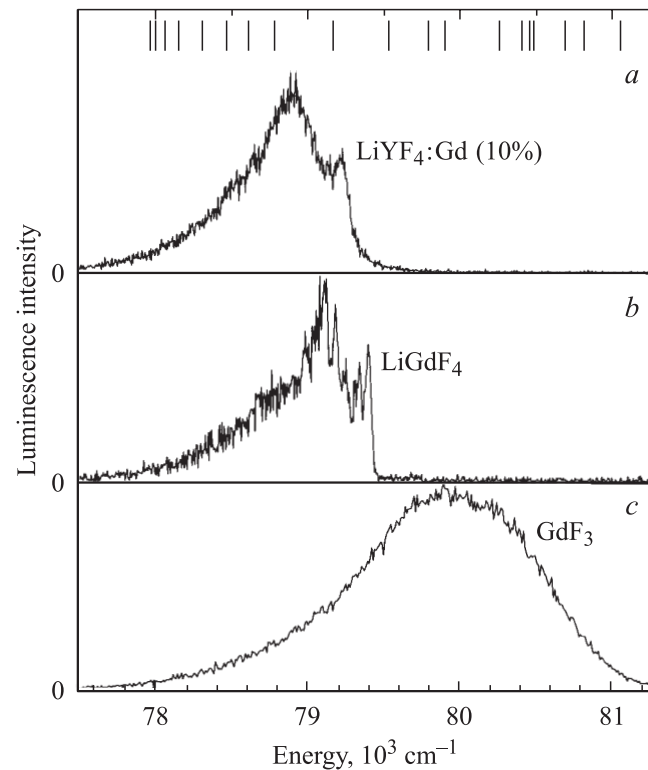


Figure 4. $\text{Gd}^{3+} d \rightarrow f$ emission of $\text{LiYF}_4:\text{Gd}^{3+}$ (10%) (a), LiGdF_4 (b) and GdF_3 (c), excited by $84\,034$ (a, b) and $85\,470\text{ cm}^{-1}$ (c). Resolution interval $\Delta\lambda_{\text{em}} = 0.8\text{ \AA}$, $T = 10\text{ K}$. Energy levels of the $\text{Gd}^{3+} 4f^7$ configuration in the range of the onset of $f \rightarrow d$ excitation [24] are included as bars.

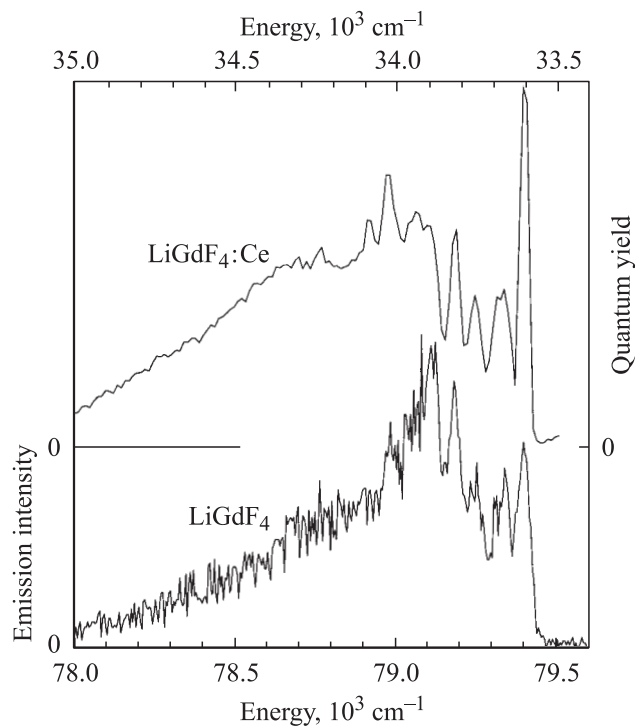


Figure 5. Comparison of $\text{Gd}^{3+} d \rightarrow f$ luminescence in LiGdF_4 (excited at $84\,034\text{ cm}^{-1}$, $\Delta\lambda_{\text{em}} = 0.8\text{ \AA}$) with a $\text{Ce}^{3+} f \rightarrow d$ excitation spectrum in $\text{LiGdF}_4:\text{Ce}^{3+}$ (0.05%) measured with $\Delta\lambda_{\text{ex}} = 2.9\text{ \AA}$. Both spectra $T = 10\text{ K}$.

as a test ion to probe electron-phonon interaction. Therefore, Ce^{3+} doped LiGdF_4 has been investigated. Due to the small Ce^{3+} concentration (0.05%), the excitation spectrum of the $\text{Ce}^{3+} d \rightarrow f$ transitions in the transparency range of the host could be measured¹ without saturation effects. It yields a fine structure with a ZPL at $33\,615\text{ cm}^{-1}$. In Fig. 5, the excitation spectrum of the $\text{Ce}^{3+} d \rightarrow f$ emission is compared with the $\text{Gd}^{3+} d \rightarrow f$ emission. The scale of the Ce^{3+} spectrum is opposite to the scale of the Gd^{3+} spectrum, and the scales are shifted in a way that the Ce^{3+} ZPL coincides with the first sharp line of the Gd^{3+} emission. The spectra agree well within the range of the pronounced lines. Therefore, the line at $79\,377\text{ cm}^{-1}$ is assigned to the ZPL of $\text{Gd}^{3+} d \rightarrow f$ emission.

The side-bands in the $\text{Ce}^{3+} f \rightarrow d$ excitation spectrum most probably originate from phonon replica. The fine structure is spread over $\sim 500\text{ cm}^{-1}$ which is in good agreement with the energy spread of phonon spectra of isostructural scheelite compounds LiLnF_4 ($Ln = \text{Y, Ho, Er, Tm, Yb}$) [29]. (The energies are not in agreement with the phonon spectra, in particular, there are no phonons with such small energies; data on LiGdF_4 are not available in the literature). The close similarity between both spectra in Fig. 5 indicates that the fine structure of the Gd^{3+}

¹ To be more precise: in $\text{LiGdF}_4:\text{Ce}^{3+}$, $\text{Ce}^{3+} d \rightarrow f$ emission is quenched by energy transfer to $4f^6 4f^* \text{Gd}^{3+}$ levels, leading to $\text{Gd}^{3+} {}^6P_{7/2} \rightarrow {}^8S_{7/2}$ emission at 311 nm. This emission was monitored while measuring the $\text{Ce}^{3+} f \rightarrow d$ excitation spectrum.

$d \rightarrow f$ emission mainly originates from vibronic modes. The smooth shape of luminescence at longer wavelengths is assigned to a superposition of vibronic modes with more than one phonon involved. The general behaviour is typical for intermediate electron-phonon coupling. A Huang–Rhys parameter $S \sim 1$ was estimated in Ref. [15].

GdF_3 emits a broad band centred at $\sim 80\,000\text{ cm}^{-1}$. It is ascribed to spin-allowed $\text{Gd}^{3+} d \rightarrow f$ emission as well. The same spectra were obtained from single crystals and powder samples. The spectral shape indicates much stronger electron-phonon coupling than in LiGdF_4 . Similar observations were reported in Ref. [7] where stronger electron-lattice coupling was found for some REF_3 compared to $\text{LiYF}_4:\text{RE}^{3+}$. In Ref. [15], an estimate of the Huang–Rhys parameter is given, $S > 5$. The shift of the $\text{Gd}^{3+} d \rightarrow f$ emission of GdF_3 to higher energies compared to LiGdF_4 is ascribed to the different coordination numbers for the Gd^{3+} ion (9 in GdF_3 , 8 in LiGdF_4), causing a smaller crystal field splitting of the d excitation in GdF_3 .

In Fig. 6, the $\text{Gd}^{3+} d \rightarrow f$ luminescence and excitation spectra are plotted together. For LiGdF_4 , the ZPL in emission coincides with the steep onset of the excitation spectrum, supporting our assignment. In the stoichiometric material, the system is optically thick, therefore no fine structure can be observed. In GdF_3 , the excitation spectrum consists of a single band which is much broader than

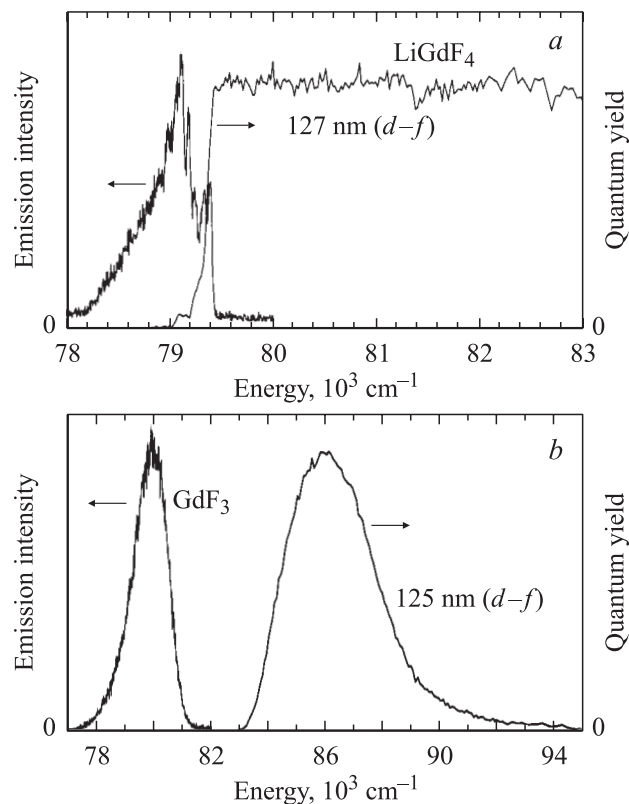


Figure 6. Comparison of (a) $\text{Gd}^{3+} d \rightarrow f$ luminescence ($\Delta\lambda_{\text{em}} = 0.8\text{ \AA}$) and excitation ($\Delta\lambda_{\text{ex}} = 1.0\text{ \AA}$) in LiGdF_4 , and of (b) $\text{Gd}^{3+} d \rightarrow f$ luminescence ($\Delta\lambda_{\text{em}} = 0.8\text{ \AA}$) and excitation ($\Delta\lambda_{\text{ex}} = 2.9\text{ \AA}$) in GdF_3 . $T = 10\text{ K}$.

the luminescence band. At first sight, this seems to indicate linear-quadratic electron-phonon coupling (different phonons coupling in the excited and the ground state [30]). Nevertheless, we hesitate to draw this conclusion because at higher energies, the system is optically thick, preventing a lineshape analysis. More than one electronic transition may be hidden in the maximum. The decrease in intensity towards higher energies may be ascribed to the onset of band-to-band transitions (it seems to be a general rule that $\text{RE}^{3+} d \rightarrow f$ luminescence is hardly excited at the onset of band-to-band excitations). The smooth onset, however, originates from strong electron-phonon coupling.

3.4. $\text{Lu}^{3+} d \rightarrow f$ luminescence. The electronic structure of Lu with its $4f^{14}$ configuration is simple. The filled f shell gives rise to only one energy level, 1S_0 . At the onset of electronic excitation, an f electron is promoted to a d orbital. The lowest excited state is an $S = 1$ state (the spin of the electron changes its direction), the next state is a singlet state (the spin keeps its direction). In other words, concerning the d excitations, we have a situation like in all other RE^{3+} ions in the second half of the series. The important difference is that in the range of $f \rightarrow d$ excitations, there are no other energy levels of Lu^{3+} available for energy transfer and subsequent quenching of the $\text{Lu}^{3+} d \rightarrow f$ emission.

The reason why $\text{Lu}^{3+} d \rightarrow f$ emission has never been detected before may arise from the fact that the energy is the highest among all RE^{3+} ions (free ion value near to $100\,000\text{ cm}^{-1}$) [16,17]. In Fig. 7, VUV luminescence spectra of a $\text{LiLuF}_4:\text{Ce}^{3+}$ crystal, a $\text{LuF}_3:\text{Ce}^{3+}$ crystal, and of LuF_3 powder are shown (see also Ref. [15]). As a consequence of the Ce^{3+} doping, the LiLuF_4 VUV luminescence was weak, therefore, the spectrum was measured at the BW3 beamline, providing high-intensity excitation by XUV photons (130 eV). LiLuF_4 emits two broad emission bands at $80\,200$ and $82\,600\text{ cm}^{-1}$. The band at $82\,600\text{ cm}^{-1}$ has a lifetime in the ns range. It is ascribed to spin-allowed $4f^{13}5d \rightarrow 4f^{14}$ emission. The band at $80\,200\text{ cm}^{-1}$ has a considerably longer lifetime and is ascribed to spin-forbidden $4f^{13}5d \rightarrow 4f^{14}$ emission. The different nature of both bands is demonstrated in Fig. 7. The open circles are time-integrated measurements, the full circles were obtained within a time-window of 0.8 ns after the excitation pulses. The assignments will be established in Sec. 3.5.

Due to the weak luminescence intensity, the excitation spectra around the threshold of $\text{Lu}^{3+} f \rightarrow d$ excitation could not be measured in $\text{LiLuF}_4:\text{Ce}^{3+}$. The moderate spectral resolution of 6 \AA and the absence of excitation spectra prevent an analysis of electron-phonon interaction. The VUV emission from the $\text{LuF}_3:\text{Ce}^{3+}$ single crystal and from the undoped LuF_3 powder consists of a broad band ($\sim 80\,500\text{ cm}^{-1}$) with slow decay (longer than the accessible range). The emission was intense enough to measure high-resolution luminescence and excitation spectra at the SUPERLUMI station. No fine structure was found, indicating strong electron-phonon coupling. The

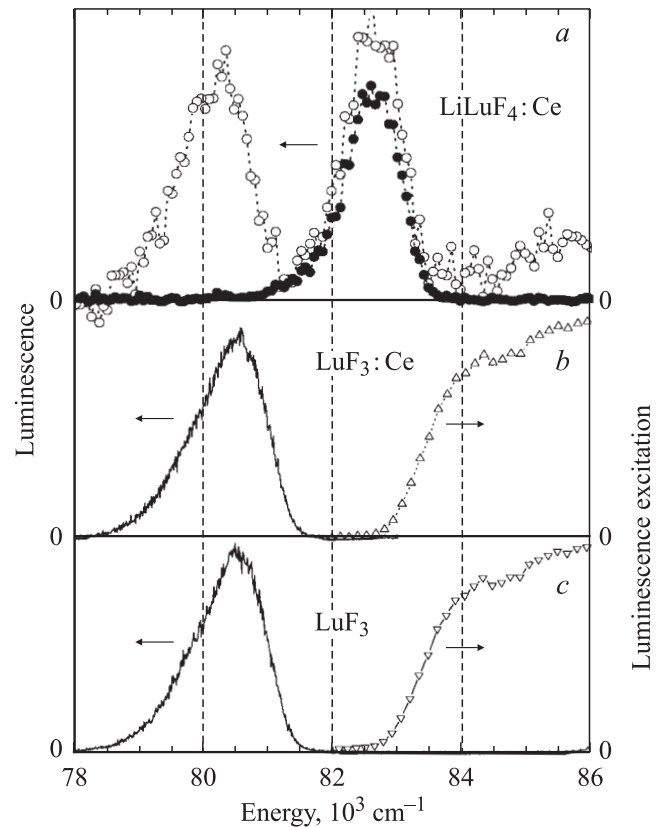


Figure 7. (a) $\text{Lu}^{3+} d \rightarrow f$ luminescence ($\Delta\lambda_{\text{em}} = 6\text{ \AA}$) from $\text{LiLuF}_4:\text{Ce}^{3+}$ excited by 130 eV photons, recorded within 0.8 ns after the excitation pulse (full circles), and time-integrated (open circles). High-resolution ($\Delta\lambda_{\text{em}} = 0.8\text{ \AA}$) luminescence excited at $86\,210\text{ cm}^{-1}$, and high-resolution excitation spectra ($\Delta\lambda_{\text{ex}} = 1.0\text{ \AA}$) of (b) $\text{LuF}_3:\text{Ce}^{3+}$ crystal and (c) LuF_3 powder at $T = 10\text{ K}$.

results of the crystal and of the powder sample agree well. On the basis of the long lifetime, the emission is ascribed to spin-forbidden $\text{Lu}^{3+} 4f^{13}5d \rightarrow 4f^{14}$ emission.

Although electron-phonon interaction of the $\text{Lu}^{3+} 4f^{13}5d$ excitation in LiLuF_4 was not analysed for reasons given above, information is obtained from Ce^{3+} emission in $\text{LiLuF}_4:\text{Ce}^{3+}$ [31]. The Ce^{3+} luminescence clearly yields a ZPL with phonon replica and a smooth low-energy sideband as it is characteristic for intermediate coupling. Moreover, in the energy range corresponding to $\text{Lu}^{3+} 4f^{14} \rightarrow 4f^{13}5d$ excitation, the excitation spectra of the Ce^{3+} emission yield pronounced sharp lines which were assigned by Kirikova et al. [31] to ZPLs of $\text{Lu}^{3+} 4f^{14} \rightarrow 4f^{13}5d$ transitions because their energies agree well with calculations based on the model of Dorenbos [16,17].

3.5. Comparison with theory. The energies of the lowest spin-allowed $5d$ states of RE^{3+} ions in a host crystal can be predicted if at least for one RE^{3+} ion in the particular crystal this value is known [16,17]. Dorenbos collected spectroscopic data of $f \rightarrow d$ transitions of RE^{3+} ions in various hosts and tabulated average values for each host. As a reference ion, Ce^{3+} has been chosen because this

Comparison between calculated and experimental values of the lowest spin-forbidden and spin-allowed $f \rightarrow d$ excitation energies of Er^{3+} , Tm^{3+} , Gd^{3+} , and Lu^{3+} ions in various fluoride-type hosts (ZPLs)

Energy		LiYF ₄ (Er ³⁺)	LiCaAlF ₆ (Tm ³⁺)	LiGdF ₄ (Gd ³⁺)	LiYF ₄ (Gd ³⁺)	LiLuF ₄ (Lu ³⁺)
$D(A)$	[15]	15 262	13 344	15 093	15 262	15 140
$\Delta E^{\text{RE,Ce}}$	[14]	30 000	29 300	45 800	45 800	49 170
$\Delta S(A)$	[15]	1597	1389		1597	1242
$\Delta E^{\text{RE},s-a}$		64 078	65 296	80 047	79 878	83 370
$\Delta E_{\text{corr}}^{\text{RE},s-a}$		63 279	64 601		79 079	82 749
$\Delta E^{\text{RE},s-f}$		61 028	62 946			
$\Delta E_{\text{corr}}^{\text{RE},s-f}$		60 229	62 251			
E^{Ce}	(ZPLs)			33 615	33 450 [31]	33 130 [31]
$\Delta E_{\text{direct}}^{\text{RE},s-a}$	(ZPLs)			79 415	79 250	82 300
ΔE^{s-a}	(ZPLs)	64 265	63 200	79 377	79 250	82 900 [31]
ΔE^{s-f}	(ZPLs)	61 020	61 410			81 550 [31]

Note. Experiment: this paper and Ref. [31]. Energies are given in cm^{-1} . Numbers which have to be compared are given in bold type.

ion has been investigated extensively. The predicted energy for the spin-allowed transition of a RE^{3+} ion is given by

$$\Delta E^{\text{RE},s-a} = 49\,340 \text{ cm}^{-1} - D(A) + \Delta E^{\text{RE,Ce}}, \quad (1)$$

where $49\,340 \text{ cm}^{-1}$ is the energy of the first $f \rightarrow d$ transition of the free Ce^{3+} ion, $D(A)$ is the crystal field depression of compound A , and $\Delta E^{\text{RE,Ce}}$ is the energy difference between the first spin-allowed $f \rightarrow d$ transition of the RE^{3+} ion and of Ce^{3+} . The basis of this approximation is the fact that the crystal field depression is not sensitive to the individual ion, $D(A)$ being an average of the $D(\text{RE}^{3+}, A)$ values for different RE^{3+} ions. The quantity $\Delta E^{\text{RE,Ce}}$ is in first approximation independent from the host and can be regarded as an intrinsic property of the respective ion. The values used by Dorenbos are average values over many compounds.

In the Table, data for part of the crystals investigated are listed. Ce^{3+} $f \rightarrow d$ excitation energies measured separately are given as well. The estimates according to Eq. (1) are then compared with the experimental results. For those cases where we measured the Ce^{3+} values, the transition energies were also calculated according to

$$\Delta E_{\text{direct}}^{\text{RE},s-a} = E^{\text{Ce}} + \Delta E^{\text{RE,Ce}}. \quad (2)$$

The calculations can be extended to the spin-forbidden $f \rightarrow d$ transitions. Dorenbos showed that the energy difference, $\Delta E_{\text{RE}}^{s-a,s-f}$, between the spin-allowed and the spin-forbidden $f \rightarrow d$ excitation energy is merely a property of the respective ion but is nearly independent from the host. The values for Er^{3+} and Tm^{3+} are 3050 and 2350 cm^{-1} . Subtracting these values from the results obtained from Eqs. (1) and (2) results in $\Delta E^{\text{RE},s-f}$, given in the Table as well.

Dorenbos treated the data in the strong coupling limit, which means, absorption and emission are approximated by

Gaussian bands, energetically separated by the Stokes shift $\Delta S(A)$. It turns out that $\Delta S(A)$ is characteristic for host A but nearly independent of the RE^{3+} ion. Consequently, the $\Delta E^{\text{RE,Ce}}$ are energetical differences between such Gaussian shaped peaks. The results from Eq. (1) should therefore not be compared with the energies of ZPLs without a further correction. Dorenbos included in Ref. [17] averaged values of $\Delta S(A)$. For linear coupling to the lattice, the ZPL would be in the middle between the absorption (excitation) and the luminescence maximum. The corrected results are then given by

$$\Delta E_{\text{corr}}^{\text{RE},s-a} = \Delta E^{\text{RE},s-a} - \frac{1}{2} \Delta S(A). \quad (3)$$

Eq. (2), however, should provide us with reliable results without any correction, if E^{Ce} is the energy of the ZPL.

In most cases, the predictions agree within 600 cm^{-1} with the experimental results [16,17]. Comparing the estimates according to Eq. (2) with the measured ZPLs (LiGdF_4 , $\text{LiYF}_4:\text{Gd}^{3+}$, LiLuF_4) yields agreement within this limit, strongly supporting our assignments. For $\text{LiYF}_4:\text{Gd}^{3+}$ and $\text{LiLuF}_4(\text{Lu}^{3+})$ the agreement between the results of Eq. (3) and experiment is also very good. For $\text{LiYF}_4:\text{Er}^{3+}$, the experimental values and the predictions differ by $800\text{--}1000 \text{ cm}^{-1}$. In the case of $\text{LiCAF}:\text{Tm}^{3+}$, the disagreement is somewhat larger. Concerning the ZPLs of the spin-forbidden $d \rightarrow f$ luminescence of $\text{LiYF}_4:\text{Er}^{3+}$ and $\text{LiCAF}:\text{Tm}^{3+}$, the agreement is better. The estimates have also been made for GdF_3 and LuF_3 [15]. Good agreement has been obtained.

4. Conclusions

High-resolution $4f^{n-1}5d \rightarrow 4f^n$ VUV luminescence spectra of fluorides doped with Gd^{3+} , Tm^{3+} , and Er^{3+} , and of stoichiometric Gd^{3+} and Lu^{3+} fluorides have been

presented. Only for GdF_3 and for LuF_3 , strong coupling of the $4f^{n-1}5d$ configuration to the lattice has been established. In all other cases, ZPLs and vibronic side bands have been observed, indicating intermediate coupling. In some cases, the coupling of RE^{3+} d levels to the lattice has been analysed with a „test ion“ (Ce^{3+}) doped into the respective matrix at a low doping level. This is a promising method which could be applied in other cases where the excitation spectra are saturated. The detailed comparison with the predictions of d excitation energies by the empirical method of Dorenbos [16,17] underlines the potential power of the method, but in addition it seems to be a worthwhile goal to extend the method to ZPLs. The observation of Gd^{3+} $d \rightarrow f$ emission requires a revision of the stand point that a dense f level system behind the d excitations generally quenches d emission. Strong influence of spin selection rules on energy transfer has been established.

The authors are indebted to A. Meijerink who provided us with numerical values for energy levels, and who made accessible to us the laser setup at the Debye Institute, University of Utrecht. Thanks are due to P. Vergeer for the assistance during the measurements in Utrecht, and to J.Y. Gesland and T.V. Ouarova for growing crystals.

References

- [1] E. Loh. *Phys. Rev.* **147**, *1*, 332 (1966).
- [2] R.T. Wegh, H. Donker, A. Meijerink. *Phys. Rev. B* **57**, *4*, R 2025 (1998).
- [3] W.M. Yen, L.R. Elias, D.L. Huber. *Phys. Rev. Lett.* **24**, *18*, 1011 (1970).
- [4] L.R. Elias, Wm.S. Heaps, W.M. Yen. *Phys. Rev. B* **8**, *11*, 4989 (1973).
- [5] Wm.S. Heaps, L.R. Elias, W.M. Yen. *Phys. Rev. B* **13**, *1*, 94 (1976).
- [6] K.H. Yang, J.A. DeLuca. *Appl. Phys. Lett.* **29**, *8*, 499 (1976).
- [7] R.T. Wegh, A. Meijerink. *Phys. Rev. B* **60**, *15*, 10 820 (1999).
- [8] J. Becker, J.Y. Gesland, N.Yu. Kirikova, J.C. Krupa, V.N. Makhov, M. Runne, M. Queffelec, T.Y. Uvarova, G. Zimmerer. *J. Lumin.* **78**, *2*, 91 (1998).
- [9] N.M. Khaidukov, N.Yu. Kirikova, M. Kirm, J.C. Krupa, V.N. Makhov, E. Negodin, G. Zimmerer. *SPIE Proc.* **4766**, 154 (2002).
- [10] J. Becker, J.Y. Gesland, N.Yu. Kirikova, J.C. Krupa, V.N. Makhov, M. Runne, M. Queffelec, T.V. Uvarova, G. Zimmerer. *J. Alloys Comp.* **275–277**, 205 (1998).
- [11] M. Schlesinger, T. Szczurek. *Phys. Rev. B* **8**, *5*, 2367 (1973).
- [12] Y. Chen, M. Kirm, E. Negodin, M. True, S. Vielhauer, G. Zimmerer. *Phys. Stat. Sol. (b)* **240**, *1*, R 1 (2003).
- [13] P. Peijzel. PhD Thesis. The University of Utrecht (2004).
- [14] M. True. PhD Thesis. The University of Hamburg (2004).
- [15] M. Kirm, J.C. Krupa, V.N. Makhov, M. True, S. Vielhauer, G. Zimmerer. *Phys. Rev. B*. In press.
- [16] P. Dorenbos. *J. Lumin.* **91**, *1–2*, 91 (2000).
- [17] P. Dorenbos. *J. Lumin.* **91**, *3–4*, 155 (2000).
- [18] G. Zimmerer. *Nucl. Instr. Meth. Phys. Res. A* **308**, *1–2*, 178 (1991).
- [19] T. Möller, G. Zimmerer. *Phys. Scripta T* **17**, 177 (1987).
- [20] C.K. Jayasankar, M.F. Reid, F.S. Richardson. *Phys. Stat. Sol. (b)* **155**, *2*, 559 (1989).
- [21] M.A. Couto dos Santos, E. Antic-Fidancev, J.Y. Gesland, J.C. Krupa, M. Lemaitre-Blaise, P. Porcher. *J. Alloys Comp.* **275–277**, 435 (1998).
- [22] G.M. Renfro, J.C. Windscheif, W.A. Sibley, R.F. Belt. *J. Lumin.* **22**, *1*, 51 (1980).
- [23] L. van Pieterse, M.F. Reid, G.W. Burdick, A. Meijerink. *Phys. Rev. B* **65**, *4*, 045 114 (2002).
- [24] A. Meijerink. Private communication.
- [25] M. True, M. Kirm, E. Negodin, S. Vielhauer, G. Zimmerer. *J. Alloys Comp.* **374**, *1–2*, 36 (2004).
- [26] W.T. Carnall, G.L. Goodman, K. Rajnak, R.S. Rana. *J. Chem. Phys.* **90**, *7*, 3443 (1989). [With supplementary tables].
- [27] J. Hölsä, R.-J. Lamminmaki, E. Antic-Fidancev, M. Lemaitre-Blaise, P. Porcher. *J. Phys.: Cond. Matter* **7**, *26*, 5127 (1995).
- [28] G.H. Dieke. In: *Spectra and Energy Levels of Rare Earth Ions in Crystals* / Ed. H.M. Crosswhite, H. Crosswhite. John Wiley & Sons, USA (1968).
- [29] S. Salaün, M.T. Fornoni, A. Bulou, M. Rousseau, P. Simon, J.Y. Gesland. *J. Phys.: Cond. Matter* **9**, *32*, 6941 (1997).
- [30] C.W. Struck, W.H. Fonger. *Understanding Luminescence Spectra and Efficiency Using W_p and Related Functions*. Springer Verlag, Berlin–Heidelberg (1991).
- [31] N.Yu. Kirikova, M. Kirm, J.C. Krupa, V.N. Makhov, E. Negodin, J.Y. Gesland. *J. Lumin.* **110**, *3*, 135 (2004).